52. SILICIFIED SEDIMENTS AND SILICA DIAGENESIS IN THE GOBAN SPUR AREA OF THE NORTHEAST ATLANTIC, LEG 80[1]

Kenichi Otsuka, Institute of Geosciences, Faculty of Science, Shizuoka University[2]

ABSTRACT

X-ray powder diffraction and optical and scanning-electron microscope analyses of sediment samples taken from four sites drilled in the Goban Spur area of the northeast Atlantic show variable diagenetic silicification of sediments at several stratigraphic horizons. The results are as follows:

1. The silicified sediments are middle Eocene at Site 548, Paleocene to lower Albian at Site 549, upper to lower Paleocene at Site 550, and lower Turonian at Site 551.
2. There are three types of these silicified sediments: nodular type in carbonate-rich host sediments, bedded type in clayey host sediments, and a type transitional between the other two.
3. Silica diagenesis is considered to progress as follows: dissolution of siliceous fossils; precipitation of opal CT in pore spaces and transformation of biogenic silica (opal A) to opal CT; development of opal CT cement; chalcedonic quartz precipitation in pore spaces and replacement of foraminiferal tests by chalcedonic quartz; and finally, transformation of opal CT to quartz, and cementation. But the strong influence of host-sediment types on diagenetic silica facies is recognized. Bedded-type silicified sediments in a clayey environment indicate a lower grade of silica diagenesis. Only very weak chalcedonic quartz formation is recognized, and there is no opal CT cementation, even in Lower Cretaceous bedded-type clayey silicified sediments.
4. The *d*(101) spacing of opal CT shows two distinct trends of ordering or decrease with burial depth; one is a rapid change, in the case of nodular silicified sediments, and the other is a more gentle shift, found in bedded silicified sediments.
5. Diagenetic silica facies of the nodular type develop as irregular concentric zones around some nodule nuclei. Also, quartz-chert nodule formation occurs at rather shallower horizons, and is discordant with the trend of decreasing *d*(101) spacing in opal CT.
6. Silicified sediments at Site 551 are shallower than at the other sites. The diagenetic silica facies suggest the probable erosion of 300 m or more of sediment at this site.
7. The zeolites clinoptilolite and phillipsite were found in the sediment samples recovered on Leg 80. Clinoptilolite occurs from the shallower levels to the deepest horizons of diagenetically silicified zones, suggesting that clinoptilolite formation is related to diagenesis of biogenic silica. Phillipsite at Site 551 (Section 551-5-2) may originate from volcanogenic material.

INTRODUCTION

Detailed studies of silicified sediments from DSDP samples have clarified the worldwide distribution of cherts and other silicified sediments in ocean basins. These studies have yielded many new insights regarding the occurrence and the nature of various silicified sediments. They have also revealed very diverse features of silica diagenesis and the formation of cherts and other siliceous sediments, such as porcellanites and diatomites (Heath, 1973; Garrison et al., 1975; Keene, 1975; Kelts, 1976; Kagami, 1979; Pisciotto, 1980; Riech, 1980; Grehin et al., 1981; Hein et al., 1981; Riech, 1981).

Previous works have identified three main diagenetic silica mineral facies in these silicified sediments: (1) X-ray-amorphous silica (opal A), (2) disordered α-cristobalite (opal CT), and (3) stable quartz (Jones and Segnit, 1971). Also, silicified sediments can be classified into two major groups: a bedded type occurring in clayey or siliceous host sediments, and a nodular type found in predominantly calcareous host sediments (Heath and Moberly, 1971; Lancelot, 1973; von Rad et al., 1978; Riech and von Rad, 1979). The bedded type in clayey or siliceous sediments has a tendency to change into so-called opal-CT porcellanites, whereas the nodular type in carbonate-rich sediments tends to be composed of quartz-cherts. Thus, the sources, processes, and other factors influencing the silica diagenesis of these two types in different host sediment facies may be different. Lancelot (1973) presented a quartz-precipitation theory based on observation of these siliceous minerals. He postulated that the different micro-environments of the host sediments control the diagenetic processes and the resultant products, and that even quartz is able to precipitate directly in a carbonate-predominant porous matrix. The diagenetic-transformation theory of silica minerals is another theory on the formation of silicified sediments, and seems to be generally accepted. Riech and von Rad (1979a) described silica diagenesis as the maturation of silica mineral from biogenic amorphous silica (opal A) to opal CT, further to quartz by dissolution–precipitation processes and/or quasi-solid–solid microstructural conversion.

These transformations of silica minerals do not always show straightforward progress, however, and the field evidence indicates very irregular occurrences in many cases. Silicic zeolites and other silicates such as clay minerals are sometimes closely related to the silica-mineral

[1] Graciansky, P. C. de, Poag, C. W., et al., *Init. Repts. DSDP*, 80: Washington (U.S. Govt. Printing Office).
[2] Address: Inst. of Geosciences, Faculty of Science, Shizuoka Univ., Japan.

diagenesis and modes of occurrence (Riech, 1979; Iijima et al., 1980). Volcanogenic silica sources may be important in some cases.

During Leg 80 of the Deep Sea Drilling Project, four sites were drilled (Sites 548, 549, 550, and 551). Each site contains zones of silicified sediments in rather limited stratigraphic intervals. A total of 414 samples (45 from Site 548, 156 from Site 549, 179 from Site 550, and 34 from Site 551), ranging from Pleistocene to Barremian, were studied by X-ray diffraction analysis. Forty-four selected samples were further investigated by thin-section examination under the optical microscope. Some samples were also investigated by scanning-electron microscope.

This chapter summarizes the results of the mineralogical and petrological analyses of the silicified sediments sampled from the four sites of Leg 80.

METHODS AND TERMS

Qualitative XRD analyses were performed on all samples, both onboard *Glomar Challenger* and in the laboratory, as already mentioned. Semiquantitative X-ray diffraction analyses were also carried out according to the method of Mitsui (1975). Values of the $d(101)$ spacing of opal CT in silicified sediments were calculated by precise XRD, using silicon as the standard material and under the condition of slow 2θ-speed (1/4° per min.). Obstacle feldspars are very scarce in Leg 80 samples in general, so the XRD peak at 22° (CuKα) is considered to be attributable almost solely to opal CT.

Diagenetic quartz was distinguished from clastic quartz grains by its characteristics in the matrix, such as its grain form, its texture (as in chalcedony aggregate), and its relation to fossil tests under the optical microscope; then its abundance was estimated mainly by visual means under the microscope, referring to XRD estimates and the background quartz contents of host sediments.

The classification and terminology of silicified sediments, designating sediments containing diagenetic silica constituents, is here based on the method proposed by von Rad et al. (1978). Amounts of three silica-mineral polymorphs—opal A, opal CT, and diagenetic quartz—were estimated by thin-section and XRD analyses, and the sediments were classified as follows (Fig. 1 legend):

1. Immature, weakly silicified sediments, containing less than 50% diagenetic silica minerals, in which opal CT predominates over quartz.
2. Porcellanite, containing more than 50% diagenetic silica, with opal CT predominant over diagenetic quartz.
3. Mature quartz-chert, containing more than 50% diagenetic quartz with the quartz heavily predominant over opal CT.

DISTRIBUTION AND OCCURRENCES OF SILICIFIED SEDIMENTS

Silicified sediments were recovered from all Leg 80 sites, but their lithofacies and occurrences vary, as do their ages, which range from 21 m.y. (lower Miocene) to 106 m.y. (lower Albian). Three types of silicified sediments are recognized in Leg 80 samples. They are a bedded type in clayey host sediments, a nodular type in calcareous host sediments, and a transitional type in both sediments.

Sediments encountered at all Leg 80 sites are more or less calcareous, composed of foraminiferal and nannofossil oozes or chalks. Nodular silicified sediments therefore occur at all sites. Excepting Site 551, their sub-bottom depths of occurrence coincide fairly well (350–440 m), despite differences in ages of host sediments (Fig. 1). The bedded silicified sediments have a relatively limited occurrence. Calcareous siltstones from Cores 549-32 to 549-48 (sub-bottom depth 483.5–626.0 m, Unit 6) contain a considerable amount of siliceous organic remains which have been transformed to opal CT. These lower to middle Albian occurrences are the oldest and deepest bedded-type silicified sediments encountered on Leg 80. Clinoptilolite at Leg 80 sites has a more extensive stratigraphic range than the silicified sediments.

Site 548

Silicified sediments recovered from Site 548 are all of the hard nodular type; the nodules are pebble size and grayish green (10GY 5/2) to dusky yellow green (5GT 5/2) or gray (N3). The host sediments are middle Eocene pale grayish green (5G 8/1-5GY 7/1), firm bioturbated nannofossil chalk. They occur in lithologic Subunit 4b, from Section 548A-19-4 to Section 548A-21,CC (sub-bottom depth 382.2–401.5 m). Most siliceous remains found in this interval are radiolarians, although a few sponge spicules are present. Clinoptilolite occurrences span a wider range than the diagenetic silica minerals, from Section 548A-14-2 to Section 548A-22-7 (middle Miocene to middle Eocene).

Site 549

Various types of silicified sediments were recovered at Site 549. They show a very wide range of ages, sub-bottom depths, and types of occurrence (from Section 549-18-1, upper Paleocene, sub-bottom depth 350.7 m, to Section 549-48-1, lower Albian, sub-bottom depth 626.3 m). These sediments correspond to sediment Subunit 3d and Units 4, 5, and 6. Subunit 3d and Units 4 and 5 are predominantly nannofossil chalks. Silicified sediments sparsely present in these chalk environments are generally of the nodular type, although some may be transitional to the bedded type.

Section 549-18-1 contains silicified sediments in the intervals 10–35 cm and 70–90 cm as layers of light brownish gray (10YR 6/2) fragmented hard breccias. These layers may be classified as the transitional type between bedded and nodular porcellanite. The host sediments are gray to light brownish gray siliceous nannofossil chalk of sediment Subunit 3d, bearing considerable amounts of sponge spicules, radiolarians, and diatoms. Sediment Unit 4 (light-colored nannofossil chalks) contains reddish brown (5YR 4/4) to olive-yellow (5Y 6/6) silicified nodules at 549-24-2, 55–65 cm; 549-24-3, 0–5 cm; 549-25-2, 50–55 cm; 549-25-3, 0–10 cm; and 549-26-1, 0–10 cm. These nodules indicate a higher maturity of silica-mineral composition. For example, a nodule from 549-24-3, 0–10 cm is composed of quartz as the only silica mineral, and shows a mature quartz-chert texture. Silicified nodular sediments were also recovered from the carbonaceous black shale of Unit 5 in 549-27-1, 24–30 cm, and from the top of Core 549-32.

The calcareous siltstone layers of sediment Unit 6 (from Cores 549-32 to 549-48) are almost uniform in lithofacies, and form bedded-type silicified sediment strata through the unit, in which the maturity of silica diagenesis is fairly low. In spite of its considerable thickness (sub-bottom depth 483.5–626.3 m), the sediment is restricted to middle to lower Albian. These weakly silicified beds are gray (N4–N8) to greenish gray (5GY 4/1)

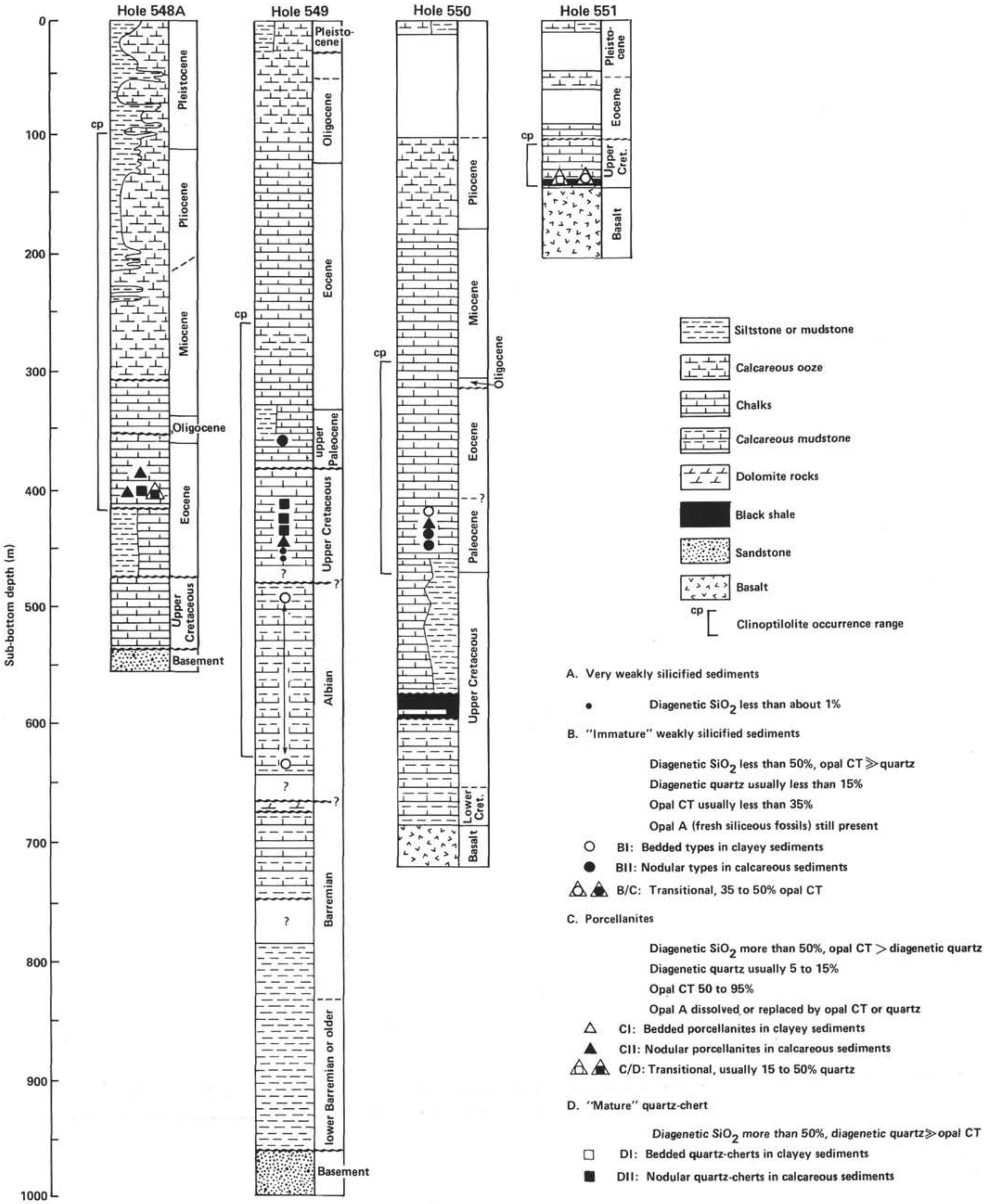

Figure 1. Lithostratigraphy and distribution of silicified sediments at Sites 548 through 551. Legend shows classification of silicified sediments.

or olive-gray (5Y 3/2) laminated, calcareous, firm siltstone with distinct bioturbated mottles. The contents of terrigenous materials such as detrital quartz and clay minerals are significant through the unit. Considerable amounts of siliceous remains (radiolarians and sponge spicules), transformed into opal CT, are scattered in a terrigenous clayey matrix.

Clinoptilolite-bearing sediments at Site 549 range from Section 549-8-2 (middle to lower Eocene, sub-bottom depth 257.7 m) to Section 549-47-4 (lower Albian, sub-bottom depth 621.1 m); that is, they appear at a shallower depth than silicified sediments, but disappear at almost the same horizon at their lower extremity.

Site 550

Siliceous biogenic remains such as radiolarians and sponge spicules are fairly abundant in some parts of the light-colored marly nannofossil chalk in the upper sediment unit, but diagenetically silicified sediments with transformed silica minerals are restricted to the interval from Section 550-35-1 (upper Paleocene, sub-bottom depth 413 m) to Section 550-38-6 (lower Paleocene, sub-bottom depth 450 m) in sediment Subunit 2b and Unit 3.

The brownish to olive-gray, marly siliceous nannofossil chalk of Subunit 2b contains a distinctive silicified hard-nodule zone, greenish gray (5GY 5/1), in the interval 550-36-2, 94–109 cm. Other remarkable nodules, pinkish to yellowish gray (5Y 8/1–5YR 8/1), occur in 550-36-1, 130–135 cm and 550-36-2, 32–46 cm, which contain abundant diagenetic dolomite crystals.

Silicified nodules also occur at 550-36-3, 144 cm; 550-37-1, 0–3 cm and 143 cm; and 550-38-6, 98–106 cm, in Subunit 3a. These nodules are generally pale brown (10YR 7/3–6/3) to brown (10YR 5/6). Some have pinkish and greenish circular features like bioturbated mottles found in adjacent sediment. Very weak haloes resulting from precipitation of diagenetically formed silica minerals also surround the nodule-bearing horizon, from Core 550-35 to Core 550-39. Clinoptilolite-bearing beds range from Core 550-22 to Core 550-41, indicating a broader zone of occurrence than diagenetic silica minerals, as observed at the previous sites.

Site 551

Silicified sediments occur in lithologic Unit 4. They are green (5G 7/2–5G 5/2) silty or siliceous chalk bands dated as Turonian. These silicified bands include fragile porcellanite–quartz-chert micronodules of granule to sand size in the host sediments of pale green (2.5Y 8/2–2.5GY 7/1) nannofossil chalk.

Black shales of sediment Unit 5 contain abundant euhedral clinoptilolite crystals as matrix, and large (0.1 mm) euhedral phillipsite cross-twinned crystals are present. Radiolarian fossils weakly transformed into diagenetic opal CT and chalcedonic quartz are also scattered in the black shale matrix, but no distinct silicified sediments were recognized. Opal-CT lepisphere precipitation is evident in foraminiferal tests in the pale gray nannofossil chalk of Unit 6, but not detectable by XRD analysis of bulk sediment. Clinoptilolite occurs more widely, from Unit 3 (lower Maestrichtian) to Unit 6 (upper Cenomanian).

MODES OF OCCURRENCE OF DIAGENETIC MINERALS

The XRD analyses of major mineralogical compositions and occurrences of diagenetic minerals are summarized in Tables 1 through 5. Silicified-sediment types in carbonate-predominant host sediments are distinctly different from those in clayey host sediments.

Diagenetic Silica Minerals in Carbonate-Predominant Sediments

Nodular porcellanites and quartz-cherts are the typical silicified sediments in the carbonate-dominant deposits such as nannofossil chalks. Very weakly silicified chalks occur around the nodules, forming a "halo zone." Siliceous fossils in the surrounding host sediments are generally not abundant, but some of these siliceous fossils around the weakly silicified "halo zones" reveal distinct dissolution pits (Plate 1, Figs. 1 and 2). These facts may indicate that dissolution of fresh biogenic silica is the initial phase of the silica diagenesis.

The next step is precipitation of opal CT in the pore spaces of the sediment matrix and within microfossils, and biogenic opal A is transformed into opal CT (Plate 2, Figs. 1–4; Plate 3, Figs. 4 and 6). The early stage of step two is manifest as the weakly silicified halo zones surrounding silicified nodules. The halo sediments have less than 1% diagenetic silica minerals, which are chiefly opal CT (Table 5).

The third step is development of opal-CT cement. The sediments of this step are represented by weakly silicified porcellaneous nodules with patchy opal-CT matrices at Site 549 (Sample 549-18-1, 22–24 cm) and Site 550 (Sample 550-38-6, 104–106 cm) (Table 5). The diagenetic silica-mineral content is 20 to 30%, most of which is opal CT.

The fourth step is replacement of foraminiferal tests by chalcedonic quartz, and precipitation of diagenetic quartz in the pore spaces of fossils and matrices (Plate 1, Fig. 5). An example of this step is in Sample 548A-21-1, 56–59 cm, where the diagenetic silica content is 64% and the ratio of opal CT to quartz is 1.4.

The fifth and the last step in silica diagenesis is the transformation of opal CT composing fossil skeletons and pore cements to quartz. Pure quartz-chert nodules are not common in Goban Spur sediment samples. One occurrence is in Sample 549-24-3, 1–3 cm. However, the transitional facies between the fourth and the fifth steps of silica diagenesis was common in the Leg 80 samples (Plate 1, Fig. 6).

Silica diagenesis in carbonate-dominant sediments seems to develop concentrically around some nodule nuclei, and it is hard to tell whether the steps from lower to higher grades of silica diagenesis are related directly to the stratigraphic position of enclosing sediments.

Dolomitic Silicified Nodules

Dolomitic porcellanite nodules were recovered in Samples 550-36-1, 133–135 cm and 550-36-2, 41–45 cm. Do-

Table 1. Lithofacies, chronostratigraphy, and XRD mineral analyses (%) of selected samples from Hole 548A.

Sample (interval in cm)	Chrono- stratigraphy	Sub-bottom depth (m)	Bulk lithology	Calcite	Quartz	Opal CT	Clinop- tilolite	Clays (smectite)
14-2, 22–24	lower Miocene	330.7	Foram. nannofossil chalk	91	4		<1	4 (3)
14-4, 90–92	lower Miocene	334.4	Foram. nannofossil chalk	90	4			6 (6)
16-2, 51–52	upper–lower Oligocene	350.0	Foram. nannofossil chalk	95	1		2	2 (1)
17-5, 85–86	upper Eocene	364.4	Foram. nannofossil chalk	89	3		4	4 (2)
18-1, 70–72	upper Eocene	367.7	Foram. nannofossil chalk	78	4		13	5 (5)
19-1, 33–35	mid. Eocene	376.7	Foram. nannofossil chalk	78	10		7	5 (2)
19-5, 50–51	mid. Eocene	383.0	Foram. nannofossil chalk	78	6		5	11 (6)
20-2, 59–60	mid. Eocene	388.1	Weakly silicified foram. nannofossil chalk	71	14	1	5	9 (5)
21-1, 56–59	mid. Eocene	396.1	Calcareous porcellanite nodule	24	28	37		11 (11)
21-1, 56–59	mid. Eocene	396.1	Outer crust of calcareous porcellanite nodule	78	11	11		
21-1, 93–95	mid. Eocene	396.5	Very weakly silicified foram. nannofossil chalk	87	13			
21-2, 74–75	mid. Eocene	397.8	Foram. nannofossil chalk	70	12		5	13 (7)
21-2, 133–136	mid. Eocene	398.4	Quartzose porcellanite nodule	5	28	29	12	27 (—)
21,CC	mid. Eocene	401.5	Outer crust of porcella- neous quartz-chert nodule	84	16			
21,CC	mid. Eocene	401.5	Edge of porcellaneous quartz-chert nodule	59	21	20		
21,CC	mid. Eocene	401.5	Porcellaneous quartz- chert nodule	12	54	34		
22-2, 91–92	mid. Eocene	407.4	Foram. nannofossil chalk	75	7		4	14 (9)
22-5, 62–65	mid. Eocene	411.6	Foram. marly nannofos- sil chalk	61	20		7	12 (—)
22-6, 106–108	lower Eocene	413.6	Marly nannofossil chalk	31	33			36 (10)
22-7, 20–22	lower Eocene	414.2	Marly nannofossil chalk	30	35		8	27 (11)
23-2, 64–65	lower Eocene	416.7	Calcareous silty mud- stone	17	27			56 (18)

Note: Dashes and blanks both mean not detected by method used.

lomite occurs as euhedral rhombic crystals in a matrix of opal CT. Veins of chalcedonic quartz cut through the matrix. Siliceous fossils, mainly radiolarians, transformed into opal CT and quartz, are scattered throughout the matrix together with dolomite crystals (Plate 3, Fig. 5).

Diagenetic Silica Minerals in Clayey Sediments

Bedded silicified sediments in clayey host sediments have a restricted occurrence in Leg 80 cores. Except for local and transitional silicified sediments, middle to lower Albian gray calcareous siltstone beds from Core 549-32 to Core 549-48 are the only major bedded silicified sediments recovered during Leg 80.

Lithofacies are almost uniform through this siltstone sediment unit. Terrigenous materials are fairly abundant, generally as silt-size detrital quartz (10–20% or so) and clay minerals (20–30%). Calcareous components make up 20 to 80% of the unit, and consist mainly of nannofossils, foraminifers, and their fragments. Siliceous biogenic components, chiefly radiolarians and sponge spicules, are commonly scattered through a terrigenous clayey matrix.

Diagenetic silica facies are also almost uniform, particularly in the upper to middle part of these weakly silicified calcareous siltstone beds. Through the beds, siliceous fossil skeletons have generally been transformed into opal CT. Opal-CT lepispheres have also been precipitated in pore spaces of microfossils and matrix. Patchy opal-CT microlenses are scattered in some places. Euhedral clinoptilolite crystals also occur in these pore spaces. Foraminiferal tests generally remain as calcite (Plate 1, Figs. 3 and 4; Plate 2, Figs. 5 and 6). In the deeper layers of this sediment unit, from Core 549-43 to Core 549-48, the grade of diagenesis is slightly higher, with precipitation of chalcedonic quartz having occurred sporadically in pore spaces. Patches or microlenses of chalcedonic quartz are present locally, and foraminiferal tests have been replaced by opal CT or quartz at the deeper levels (Table 5).

The content of diagenetic silica minerals ranges from less than 1% to 30% in samples from this bedded silici-

Table 2. Lithofacies, chronostratigraphy, and XRD mineral analyses (%) of selected samples from Hole 549.

Sample (interval in cm)	Chrono-stratigraphy	Sub-bottom depth (m)	Bulk lithology	Calcite	Quartz	Opal CT	Clinop-tilolite	Clays (smectite)
2-2, 44–46	upper Eocene	200.5	Nannofossil chalk	82	6			12 (7)
8-2, 72–73	mid. Eocene	257.7	Nannofossil chalk	69	10		2	19 (10)
9-2, 56–57	mid. Eocene	267.1	Nannofossil chalk	74	5		4	17 (8)
10-5, 51–52	lower Eocene	281.0	Marly nannofossil chalk	72	7		9	12 (9)
11-2, 59–60	lower Eocene	286.1	Marly nannofossil chalk	15	26		5	54 (22)
14-2, 55–56	lower Eocene	314.6	Marly nannofossil chalk	63	5		2	30 (20)
15-2, 56–57	lower Eocene	324.1	Calcareous claystone	39	17		2	42 (19)
17-2, 79–80	upper Paleocene	343.3	Siliceous marly nannofossil chalk	53	7		1	39 (34)
18-1, 22–24	upper Paleocene	350.7	Weakly silicified calcareous porcellanite nodule	55	3	29		13 (9)
18-2, 96–99	upper Paleocene	353.0	Siliceous nannofossil chalk	94	6			
18-2, 96–99	upper Paleocene	353.0	Clayey concretion in siliceous nannofossil chalk	33	2			65 (58)
19-2, 41–42	upper Paleocene	361.9	Siliceous marly nannofossil chalk	63	5			32 (29)
20-5, 9–10	upper Paleocene	375.6	Siliceous marly nannofossil chalk	57	8		10	25 (19)
21-2, 19–20	lower Paleocene	380.7	Nannofossil chalk	73	5		6	16 (13)
22-1, 2–3	Maestrichtian	388.5	Clayey concretion in nannofossil chalk	20	29		6	45 (7)
22-2, 105–106	Maestrichtian	391.1	Nannofossil chalk	95	<1		3	2 (1)
22,CC	Maestrichtian	395.8	Nannofossil chalk	79	3			18 (7)
23-2, 54–55	Maestrichtian	400.0	Nannofossil chalk	94	<1		3	3 (2)
24-2, 18–19	Campanian	409.2	Nannofossil chalk	92	2		3	3 (2)
24-3, 1–3	Campanian	410.5	Quartz-chert nodule		≈100			
25-2, 24–25	Santonian–Coniacian	418.8	Nannofossil chalk	86	5	2	3	4 (2)
25-2, 39–41	Santonian–Coniacian	418.9	Nannofossil chalk	93	7			
25-2, 53–55	Santonian–Coniacian	419.0	Calcareous porcellaneous quartz-chert	11	50	39		
26-1, 8–9	Turonian	426.6	Porcellaneous quartz-chert	6	60	34		
26-1, 24–25	Turonian	426.8	Nannofossil chalk	84	5	1	4	6 (4)
26-1, 46–48	Turonian	427.0	Nannofossil chalk	81	5		5	9 (3)
27-1, 29–30	Turonian–Cenomanian	436.3	Calcareous porcellanite in black shale	31	15	49	5	
27-1, 42–43	Turonian–Cenomanian	436.4	Laminated black carbonaceous shale	3	26		27	44 (32)
28-1, 73–74	Cenomanian	446.2	Nannofossil chalk	69	12		9	10 (5)
28-2, 25–26	Cenomanian	447.3	Nannofossil chalk	75	9	2	8	6 (4)
28-2, 30–32	Cenomanian	447.3	Foram. nannofossil chalk	72	12		10	6 (6)
29-1, 19–20	Cenomanian	455.2	Nannofossil chalk	67	15	7	5	6 (4)
32-1, 17–18	mid. Albian	483.7	Gray calcareous siltstone	22	27	25	6	20 (6)
32-1, 35–37	mid. Albian	483.9	Gray calcareous siltstone	34	19	20	7	20 (—)
32,CC	mid. Albian	484.1	Gray calcareous siltstone	46	22	11	7	14 (5)
34-1, 52–53	mid. Albian	503.0	Gray calcareous siltstone	51	19	16	4	10 (2)
34-1, 55–56	mid. Albian	503.1	Gray calcareous siltstone	63	15	7	8	7 (—)

Table 2. (Continued).

Sample (interval in cm)	Chrono-stratigraphy	Sub-bottom depth (m)	Bulk lithology	Calcite	Quartz	Opal CT	Clinop-tilolite	Clays (smectite)
35-1, 37–39	mid. Albian	512.4	Gray calcareous siltstone	35	21	30	7	7 (—)
35-1, 139–141	mid. Albian	513.4	Gray calcareous siltstone	26	23	20	13	18 (9)
35,CC (2–3)	mid. Albian	513.7	Gray calcareous siltstone	66	10		5	19 (6)
36-1, 5–7	Albian	521.6	Gray calcareous siltstone	73	12	9	6	
36-1, 15–17	Albian	521.7	Laminated calcareous sandy siltstone	36	26		21	17 (—)
36-1, 20–21	Albian	521.7	Gray calcareous siltstone	49	25	6	5	15 (5)
37-1, 20–21	Albian	522.7	Gray calcareous siltstone	19	18	8	15	39 (8)
37-1, 31–32	Albian	522.8	Gray calcareous siltstone	23	19		21	37 (15)
37-2, 36–38	Albian	524.4	Gray calcareous siltstone	43	12		11	34 (8)
38-1, 34–35	Albian	531.4	Nannofossil chalk	83	5	3	2	7 (2)
39-1, 6–7	Albian	540.6	Gray calcareous siltstone	32	22	9	9	28 (9)
40-1, 7–8	Albian	550.1	Gray calcareous siltstone	33	21	9	8	29 (9)
42-1, 38–39	Albian	569.4	Light gray calcareous siltstone	72	9	1		18 (5)
42-2, 36–37	Albian	570.9	Gray calcareous siltstone	41	21	11	6	21 (5)
42-2, 38–40	Albian	570.9	Gray calcareous siltstone	44	11	8	10	27 (7)
43-2, 88–90	Albian	580.9	Gray calcareous siltstone	28	32	7	3	30 (10)
43-3, 127–130	Albian	528.8	Gray calcareous siltstone	30	16	8	10	36 (8)
44-2, 110–111	Albian	590.6	Gray calcareous siltstone	58	15	11	2	14 (6)
44-3, 141–143	Albian	592.4	Gray calcareous siltstone	37	18		10	35 (9)
45-3, 40–41	Albian	600.9	Gray calcareous siltstone	40	24	16	3	17 (7)
45-3, 130–133	Albian	601.8	Gray calcareous siltstone	35	15	6	7	37 (7)
46-3, 31–33	Albian	610.3	Gray calcareous siltstone	56	14	6	7	17 (—)
46-4, 91–92	Albian	612.4	Gray calcareous siltstone	32	20	11	7	30 (10)
47-1, 46–47	Albian	617.0	Gray calcareous siltstone	32	22	10	5	31 (8)
47-2, 92–94	Albian	618.9	Gray calcareous siltstone	47	17			36 (9)
47-3, 84–86	Albian	620.4	Gray calcareous siltstone	46	24	8		22 (9)
47-4, 14–17	Albian	621.2	Gray calcareous siltstone	39	27	4	7	22 (8)
47-4, 24–26	Albian	621.3	Gray calcareous siltstone	71	9			20 (7)
47-4, 72–73	Albian	621.7	Gray calcareous siltstone	40	32			28 (11)
48-1, 33–34	Albian	626.3	Gray calcareous siltstone	49	24	5		22 5

Note: Dashes and blanks both mean not detected by method used.

fied siltstone. Almost all of the diagenetic silica is opal CT, but diagenetic quartz appears in the deeper parts of the unit. These diagenetic facies correspond to the second to fourth steps of silica diagenesis in the case of carbonate-predominant sediments, previously outlined. But development of opal-CT cement, the third step, is poor in these clayey sediments. Slight but detectable progression of diagenetic silica facies with increase in sub-bottom depth is a characteristic feature in the clayey sediments.

OPAL-CT LATTICE SPACING

The *d*(101) spacing of opal CT is considered a good index of the degree of silica diagenesis. Murata and Larson (1975) recognized a decrease in the *d*(101) spacing of opal CT with burial depth in the Monterey Shale, and attributed this to a progressive diagenetic ordering. Such a decrease or ordering of *d* spacing of opal CT with burial depth has been reported by some other investigators (von Rad et al., 1978; Iijima et al., 1980).

Table 3. Lithofacies, chronostratigraphy, and XRD mineral analyses (%) of selected samples from Hole 550.

Sample (interval in cm)	Chrono-stratigraphy	Sub-bottom depth (m)	Bulk lithology	Calcite	Dolomite	Quartz	Opal CT	Opal A	Clinop-tilolite	Clays (smectite)
21-3, 75	lower Miocene	283.7	Marly nannofossil chalk	79		7				14 (—)
22-2, 18–19	lower Miocene	291.2	Marly nannofossil chalk	58		11			2	29 (12)
23-2, 47–48	lower miocene	301.0	Marly nannofossil chalk turbidite layer	58		11		7	2	22 (11)
24-4, 104	lower Eocene	314.0	Claystone	6		14			6	73 (21)
24-4, 108	lower Eocene	314.1	Calcareous claystone	24		18				58 (27)
25-1, 38–39	lower Eocene	318.4	Marly nannofossil chalk	49		13			5	33 (15)
28-1, 46–47	lower Eocene	347.0	Marly nannofossil chalk	58		10				32 (18)
28-1, 68–69	lower Eocene	347.2	Marly nannofossil chalk	65		7			4	24 (14)
29-2, 68–69	lower Eocene	358.2	Marly nannofossil chalk	76		4			<1	20 (11)
34-4, 118	upper Paleocene	409.2	Siliceous marly nannofossil chalk	65		13				22 (12)
34-5, 118	upper Paleocene	410.7	Calcareous claystone	41		13				46 (31)
34-5, 119	upper Paleocene	410.7	Calcareous sandy claystone	46		19			9	26 (18)
34-5, 145	upper Paleocene	410.9	Claystone			13			10	77 (60)
35-1, 23–24	upper Paleocene	413.2	Weakly silicified calcareous mudstone	57		3	13		6	21 (21)
35-1, 136	upper Paleocene	414.4	Calcareous mudstone	50		12				38 (38)
35-2, 12–13	upper Paleocene	414.6	Claystone	10		5				85 (73)
35-5, 12–13	upper Paleocene	419.1	Claystone	3		12				85 (70)
35-5, 69–71	upper Paleocene	419.7	Nannofossil-bearing siliceous claystone	25		11				64 (54)
35-5, 87–89	upper Paleocene	419.9	White foram. marly nannofossil chalk	57		7				36 (20)
35-5, 87–89	upper Paleocene	419.9	Brown siliceous claystone	30		15				55 (39)
35-5, 105	upper Paleocene	421.0	Calcareous claystone	42		14			6	39 (31)
35-5, 138	upper Paleocene	421.3	Green to pinkish streak of claystone	11		2				87 (84)
36-1, 12–15	upper Paleocene	422.6	Laminated calcareous mudstone	47		4			10	38 (38)
36-1, 13–15	upper Paleocene	422.6	Calcareous claystone	13		18				69 (69)
36-1, 132–135	upper Paleocene	423.8	Porcellaneous dolomite nodule	7	68	5	20			
36-1, 134	upper Paleocene	423.8	Outer part of porcellaneous (dolomite) nodule	22		5	57			16 (16)
36-2, 41–45	upper Paleocene	424.4	Dolomitic porcellanite nodule		12	8	67			13 (13)
36-2, 41–45	upper Paleocene	424.4	Outer crust of dolomitic porcellanite nodule	5		3	18			73 (73)
36-2, 134	upper Paleocene	425.3	Claystone	11		31			30	28 (17)
36-3, 126	upper Paleocene	426.8	Pink mottle in marly nannofossil chalk	39		2				59 (39)
37-1, 0–3	upper Paleocene	432.0	Brownish calcareous porcellanite nodule	23		17	60			
37-1, 0–3	upper Paleocene	432.0	White part of calcareous porcellanite nodule	81		6	13			
37-1, 143	upper Paleocene	433.4	Green-pink siliceous concretion in nannofossil chalk	32		5	19			44 (44)
37-2, 31–32	upper Paleocene	433.8	Marly nannofossil chalk	53		3	3		7	34 (34)
37-2, 140	upper Paleocene	434.9	Green clayey concretion in marly nannofossil chalk	14						86 (75)

Table 3. (Continued).

Sample (interval in cm)	Chrono-stratigraphy	Sub-bottom depth (m)	Bulk lithology	Calcite	Dolomite	Quartz	Opal CT	Opal A	Clinop-tilolite	Clays (smectite)
37-4, 31–32	upper Paleocene	436.8	Marly nannofossil chalk	69		3	5			23 (21)
38-6, 70	lower Paleocene	449.7	White siliceous fossil-bearing marly nannofossil chalk	64		5			16	15 (12)
38-6, 102	lower Paleocene	450.0	Brown concretion of weakly silicified siliceous marly nannofossil chalk	55		9	14		6	16 (13)
38-6, 104–106	lower Paleocene	450.1	White concretion of weakly silicified siliceous marly nannofossil chalk	44		9	23		13	11 (—)
38-6, 104–106	lower Paleocene	450.1	Brown concretion of weakly silicified siliceous marly nannofossil chalk	64		5	12		11	8 (—)
39-2, 35–37	lower Paleocene	452.9	Marly siliceous nannofossil chalk	67		5			17	11 (4)
39-5, 92–93	lower Paleocene	457.9	Nannofossil chalk	92		2			<1	5 (3)
41-2, 55–56	upper Maestrichtian	472.1	Marly nannofossil chalk	78		2			9	11 (9)
42-1, 9–10	upper Maestrichtian	479.1	Sandy calcareous turbidite	45		11				44 (21)

Note: Dashes and blanks both mean not detected by method used.

Figure 2 shows the changes of *d* spacing of opal CT with sub-bottom depth for silicified sediment samples from all sites drilled during Leg 80. The range of the *d*(101) spacing of opal CT is from 4.115 to 4.069 Å, and the decrease or ordering of *d* spacing with sub-bottom depth is shown by two different trends of clusters, although a few exceptions occur. The two clusters correspond to the nodular and bedded types of silica diagenesis, respectively. The *d* spacing decreases rapidly at shallower horizons (from 395 to 450 m) in nodular-type silicified sediments than in bedded silicified sediments. The *d* spacing decreases more gradually at deeper horizons (from 480 to 620 m) in the bedded silicified sediments of Site 549.

These trends illustrate the difference in silica diagenesis between nodular and bedded types. The *d* spacings fluctuate considerably, and do not show simple linear trends with burial depth. Thus, the overall trend is not always obvious if a limited number of samples are examined separately, particularly in the case of sporadic nodular-type silicified sediments. However, the trend of decreasing *d* spacings for the nodular type may also indicate that unconformities do not severely perturb the relative burial depths at Sites 548, 549, and 550 since formation of the silicified nodules. Silicified sediments do occur at shallower depths at Site 551 than at the other sites, judging from the diagenetic silica facies.

Another noteworthy fact is that the spacings of opal CT in mature quartzose chert nodules do not fall in a narrow-spacing group. Rather, opal CT in quartzose chert nodules has wide *d* spacings. This may indicate that quartz precipitation or mature quartz-chert formation is a different phenomenon from opal-CT ordering, and that the relation between these two silica minerals is not defined by a simple replacement of opal CT by quartz after the opal-CT lattice becomes ordered.

ZEOLITES

Clinoptilolite

X-ray diffraction analyses show occurrences of clinoptilolite over a very wide range of age, depth, and host-sediment type (Fig. 1, Tables 1–5). Clinoptilolite-bearing sediments from Leg 80 sites are hemipelagic to pelagic chalks, calcareous siltstones, calcareous sandy claystones, and black zeolitic shales. Nearly all of these sediments are devoid of tuff and volcanic glass shards, except for the black shales of Site 551 (Section 551-5-2). Stratigraphically, clinoptilolite occurs from shallower to lower levels than the zones of diagenetically silicified sediments. These facts may indicate some relationship between clinoptilolite and silica diagenesis; they also suggest that clinoptilolite originates as a precipitate from a biogenic silica solution. Clinoptilolite occurs generally as distinct euhedral crystals or aggregates of crystals in pore spaces. In the black zeolitic shales of Section 551-5-2, clinoptilolite constitutes 20 to 35% of the rock as fine matrix in both the black and white laminae, accompanied by sporadic euhedral cross-twinned phillipsite and radiolarians transformed into opal CT and quartz (Plate 3, Figs. 1 and 2).

Phillipsite

Phillipsite occurs only in the black shales of Section 551-5-2, as sporadic large (30–100 μm) euhedral cross-twinned crystals in a fine matrix of clinoptilolite and clay minerals (Tables 4 and 5). Riech and von Rad (1979a) noted that phillipsite commonly occurs as an alteration

Table 4. Lithofacies, chronostratigraphy, and XRD mineral analyses (%) of selected samples from Hole 551.

Sample (interval in cm)	Chrono-stratigraphy	Sub-bottom depth (m)	Bulk lithology	Calcite	Quartz	Opal CT	Clinop-tilolite	Clays (smectite)	Phillip-site
2-1, 2	Maestrichtian	104.0	Foram. nannofossil ooze	92	8				
2-2, 135-136	Maestrichtian	106.9	Calcareous clay	89			3	8 (6)	
3-2, 96-97	lower Maestrichtian	116.0	Marly nannofossil ooze	90	1		2	6 (5)	
3-3, 139	lower Maestrichtian	117.9	Marly nannofossil ooze	88	4			7 (—)	
4-2, 54	upper Campanian	125.5	Nannofossil chalk	95	5				
4-2, 119-120	upper Campanian	126.2	Nannofossil chalk	87	1		7	5 (3)	
5-1, 14	lower Turonian	132.6	Nannofossil chalk with white mottles	76	6		6	12 (5)	
5-1, 30	lower Turonian	132.8	Olive clay band					100 (75)	
5-1, 48-49	lower Turonian	133.0	Laminated calcareous mudstone	36	9			55 (55)	
5-1, 53-54	lower Turonian	133.0	Laminated nannofossil chalk	64	8		5	23 (13)	
5-1, 114	lower Turonian	133.6	Laminated nannofossil chalk	73	5		7	15 (5)	
5-2, 3-5	lower Turonian	134.0	Marly silicified nannofossil chalk with porcellaneous chert patches	40	40	20			
5-2, 6	lower Turonian	134.0	Marly silicified nannofossil chalk with porcellaneous chert patches	42	38	16	3		
5-2, 20	lower Turonian	134.2	Nannofossil chalk	82	4		5	9 (6)	
5-2, 49-51	lower Turonian	134.5	Marly silicified nannofossil chalk with porcellaneous chert patches	4	36	43	11	5 (5)	
5-2, 50-53	lower Turonian	134.5	Marly silicified nannofossil chalk with porcellaneous chert patches	35	32	25		8 (—)	
5-2, 56	lower Turonian	134.6	Marly nannofossil chalk	42	15		25	17 (—)	
5-2, 57-58	lower Turonian	134.6	Green and black granular porcellaneous cherty mud	29	23	30	17	—	
5-2, 70	lower Turonian	134.7	Black carbonaceous zeolitic clay	—	18		37	45 (—)	
5-2, 79-81	lower Turonian	134.8	Black zeolitic carbonaceous mudstone with zeolitic clay lamina	6	12		29	17 (6)	35
5-2, 91-92	lower Turonian	134.9	Marly chalk in black carbonaceous zeolitic clay	44	13		26	17 (6)	
5-2, 101-103	lower Turonian	135.0	Black zeolitic carbonaceous mudstone, zeolitic clay lamina	9	12		22	14 (—)	40
5,CC	lower Turonian	135.3	Black carbonaceous zeolitic clay	—	16		34	43 (—)	6
6-1, 13-14	upper Cenomanian	142.2	Foram. nannofossil chalk	71	3		15	7 (2)	
6-2, 76	upper Cenomanian	144.3	Foram. nannofossil chalk	93	3		4		
6-2, 84-86	upper Cenomanian	144.4	Foram. nannofossil chalk	74	5		10	11 (3)	

Note: Dashes and blanks both mean not detected by method used.

product of volcanic glass and other pyroclastics. Thus, at least part of the black zeolitic shales of Site 551 may have originated as volcanogenic materials.

DISCUSSION AND SUMMARY

Von Rad et al. (1978) stated that the ratio of opal-CT content to diagenetic-quartz content serves as a rough measure of the mineralogical maturity of silicified sediments. The plot of this ratio versus age of Leg 80 samples shows some fluctuations from the plot of von Rad et al. (1978), particularly for the samples older than Lower Cretaceous (Fig. 3). Weakly silicified clayey sediments in which opal CT is the only diagenetic silica mineral occur in Lower Cretaceous sediments of Site 549.

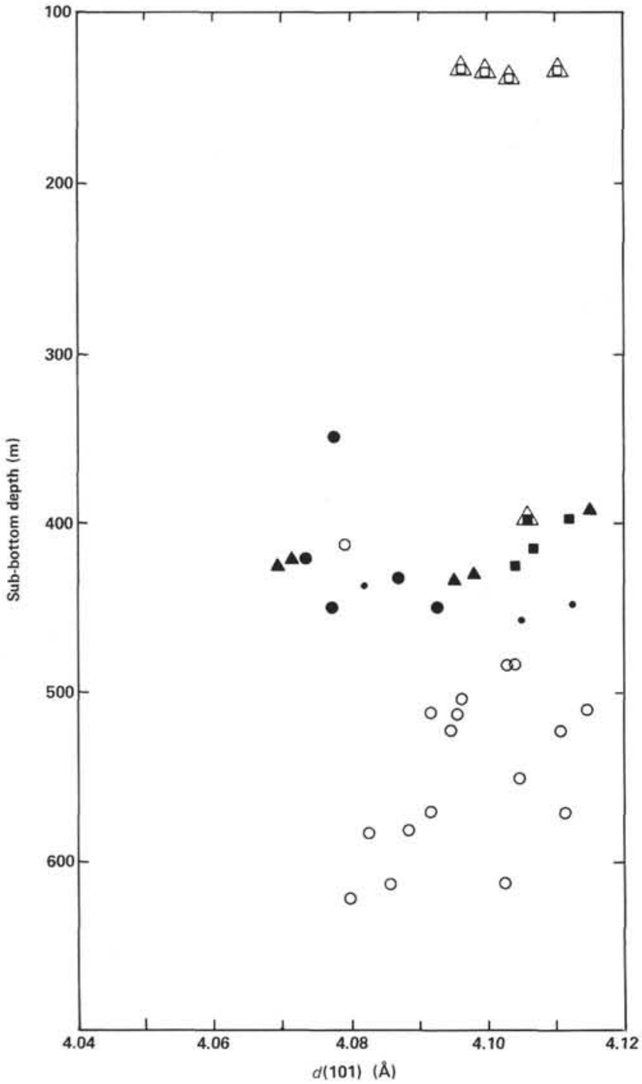

Figure 2. Relation of $d(101)$ spacing of opal CT and burial depth of silicified sediments at Leg 80 sites (symbols for silicified sediment types as in Fig. 1 legend).

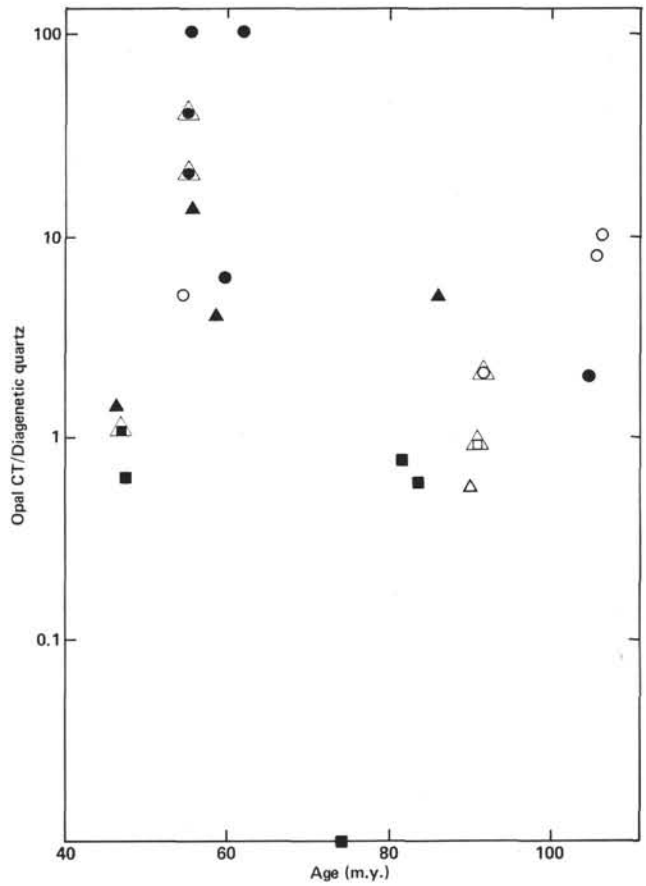

Figure 3. The ratio of opal-CT content to diagenetic-quartz content as a function of sample age for the various types of silicified sediment (symbols for silicified sediment types as in Fig. 1 legend).

Further, the ratio of opal-CT content to diagenetic-quartz content does not seem to decrease in older sediments. Rather, quartz-cherts occur in younger host sediments.

Figure 4 shows diagenetic silica facies as a function of host sediment age and sub-bottom depth. The lines dividing the mineral fields are taken from Riech and von Rad (1979a). The distribution pattern of Leg 80 samples is not very different from their diagenetic-mineral fields. The distribution of chert nodules from Site 548 in the field of opal A and opal CT is one anomaly; and the bedded, weakly silicified sediments from Site 549 (Lower Cretaceous), with opal CT as almost the only diagenetic silica mineral, plot in the field of opal CT and quartz and constitute another anomaly in Figure 4. This diagenetic facies indicates a little more immature stage of diagenesis than that suggested by Riech and von Rad (1979a). The anomalies may be attributed to the irregular and overlapping stages of silica diagenesis, varying between the nodular types in carbonate sediments and bedded types in clay matrices.

As already shown by Figures 2 and 3, the nodular type of silicified sediment in carbonate-dominant host sediments tends to show rapid silica diagenesis, whereas the diagenetic change in the bedded type of silicified sediments in clayey host strata occurs more slowly. Thus, even Lower Cretaceous sediments have immature facies with high ratios of opal-CT content to diagenetic-quartz content in the case of bedded silicified sediments in clayey matrices.

Lancelot (1973) noted that foreign cations in silica solutions should be relatively abundant in clayey sediments and thereby favor the formation of diagenetic opal CT rather than quartz. With regard to opal-CT cement formation, however, this theory is not so simply applied to the bedded clayey silicified sediments of Site 549, in which silica cementation is poor.

The ordering or maturation of the opal-CT $d(101)$ spacing takes place rapidly in carbonate sediments, but is slow in clayey deposits (Fig. 2). It should be noted, however, that irregularities in the ordering or opal-CT d spacings are particularly apparent in nodular-type silicified sediments in carbonate host sediments. The relation between changes in the opal-CT d spacing and the silicified sediment type also suggests that quartz-chert formation is not directly related to the ordering trend of opal-CT d spacings, especially for nodular-type cherts. Nodules at shallower depths have wide, disordered opal-

Table 5. Lithofacies, chronostratigraphy, and diagenetic silica facies determined by optical and scanning-electron microscopes, selected Leg 80 silicified sediments.

Sample (interval in cm)	Chrono-stratigraphy	Sub-bottom depth (m)	Host rock	Lithology of investigated sample	Mode of occurrence of diagenetic minerals: Fossil skeleton	Mode of occurrence of diagenetic minerals: Pore filling of fossil	Mode of occurrence of diagenetic minerals: Matrix	Diagenetic silica (%)	Opal CT / Diag. Qtz	Remarks
548A-18-1, 70–72	upper Eocene	367.7	Foram. nannofossil chalk	Foram. nannofossil chalk	Forams. → only calcite	Forams. → {clinoptilolite, clay}		—	—	Glauconite-bearing
548A-19-1, 33–35	mid. Eocene	376.9	Foram. nannofossil chalk	Foram. nannofossil chalk	Forams. → only calcite	Forams. → {clinoptilolite, clay}	Pore space → clinoptilolite Microlens of quartz-chert	≪1	—	
548A-21-1, 56–59	mid. Eocene	396.1	Foram. nannofossil chalk	Calcareous porcellanite nodule	Forams. → quartz Sponge spicules → opal CT	Forams → {opal CT lep., quartz, pyrite}	Opal CT	64	1.4	Pyrite spherules, glauconite
548A-21-1, 93–95	mid. Eocene	396.5	Foram. nannofossil chalk	Very weakly silicified foram. nannofossil chalk	Forams. → only calcite	Forams. → {(clinoptilolite), (opal CT), clay}	Microlens of opal CT and clinoptilolite	<1	∞	Glauconite
548A-21-2, 133–136	mid. Eocene	398.4	Foram. nannofossil chalk	Quartzose porcellanite nodule	Forams. → quartz Sponge spicules, Rads. → {opal CT, quartz}	Forams. → {opal CT lep., quartz, clinoptilolite} Rads. → {opal CT, quartz}	Opal CT Microlens of chalcedonic quartz	56	1.1	
548A-22-5, 62–65	mid. Eocene	411.6	Foram. marly nannofossil chalk	Foram. marly nannofossil chalk	Forams. → only calcite	Forams. → clinoptilolite	Pore space → clinoptilolite	—	—	Glauconite
549-18-1, 22–24	upper Paleocene	350.7	Siliceous nannofossil chalk	Weakly silicified calcareous porcellanite nodule	{Rads., Sponge spicules, Diatoms} → opal CT Forams. → only calcite	{Rads., Sponge spicules, Diatoms} → opal CT Forams. → {opal CT, quartz}	Patches of opal CT	30	≈100	
549-18-2, 96–99	upper Paleocene	353.0	Siliceous nannofossil chalk	Clayey concretion in siliceous nannofossil chalk	{Rads., Sponge spicules, Diatoms} → fresh, partly dissolved			—	—	
549-24-3, 1–3	Campanian	410.5	Nannofossil chalk	Quartz-chert nodule	{Forams., Rads., Sponge spicules, Diatoms} → quartz, opal CT at nodule edge	{Forams., Rads., Sponge spicules, Diatoms} → {quartz, opal CT at nodule edge}	Quartz Edge of nodule → opal CT	≈100	≈0.01	Pyrite spherules
549-25-2, 39–41	Santonian–Coniacian	418.9	Nannofossil chalk	Nannofossil chalk	Forams. → only calcite (Rads. → opal CT)	Forams. → {opal CT, clinoptilolite} (Rads. → opal CT)	Patches of opal CT	1	∞	
549-25-2, 53–55	Santonian–Coniacian	419.0	Nannofossil chalk	Calcareous porcellaneous quartz-chert	Forams. → {quartz, opal CT, partly calcite} Rads. → {quartz, opal CT}	Forams. → {quartz, opal CT} Rads. → {quartz, opal CT}	Opal CT and quartz as matrix Patches of chalcedonic quartz	88	0.80	
549-26-1, 8–9	Turonian	426.6	Nannofossil chalk	Porcellaneous quartz-chert	{Rads., Diatoms, Sponge spicules, Forams.} → {opal CT, quartz}	{Rads., Diatoms, Sponge spicules, Forams.} → {opal CT, quartz}	Opal CT and quartz as matrix Patches of chalcedonic quartz and opal CT	93	0.60	
549-28-2, 30–32	Cenomanian	447.3	Foram. nannofossil chalk	Foram. nannofossil chalk	Forams. → only calcite (Rads. → quartz)	Forams. → {clinoptilolite, opal CT} (Rads. → quartz)	Patches of opal CT or chalcedonic quartz	<1		Glauconite
549-32-1, 35–37	mid. Albian	483.9	Siliceous fossil-bearing calcareous siltstone	Weakly silicified siliceous fossil-bearing calcareous siltstone	Forams. → {calcite, partly quartz, opal CT)} {Rads., Sponge spicules, Diatoms} → opal CT	Forams. → {opal CT, clinoptilolite, micritic calcite} {Rads., Sponge spicules, Diatoms} → opal CT	Patches of opal CT and clinoptilolite Opal CT matrix	20	∞	

549-34-1, 55–56	mid. Albian	503.1	Siliceous fossil-bearing calcareous siltstone	Weakly silicified siliceous fossil-bearing calcareous siltstone	Forams. → partly opal CT Rads., Sponge spicules → opal CT	Forams. → {opal CT, calcite} Rads., Sponge spicules → opal CT	Patches of opal CT and clinoptilolite in pore space	7	∞	Glauconite
549-35-1, 37–39	mid. Albian	512.4	Siliceous fossil-bearing calcareous siltstone	Porcellaneous silicified siliceous fossil-bearing calcareous siltstone	Forams. → {calcite, partly dissolved} Sponge spicules, Rads. → opal CT or partly dissolved	Forams. → {opal CT, clinoptilolite} Rads., Sponge spicules → opal CT → clinoptilolite	Patches of opal CT and clinoptilolite in pore space	30	∞	
549-36-1, 15–17	mid.–lower Albian	521.7	Laminated calcareous siltstone	Laminated calcareous sandy siltstone	Forams. → only calcite Rads., Sponge spicules → opal CT	Forams. → calcite Rads., Sponge spicules → opal CT	Clinoptilolite in pore spaces	< 1	∞	
549-42-2, 38–40	mid.–lower Albian	570.9	Laminated calcareous siltstone	Laminated weakly silicified siliceous fossil-bearing calcareous siltstone	Rads., Sponge spicules → opal CT Forams. → only calcite	Rads., Sponge spicules → opal CT Forams. → {calcite, opal CT, clinoptilolite}	Patches of opal CT and clinoptilolite and microlens of quartz	9	8	Pyrite spherules
549-43-3, 127–130	mid.–lower Albian	582.8	Laminated calcareous siltstone	Laminated weakly silicified siliceous fossil-bearing calcareous siltstone	Forams. → {calcite, partly quartz and opal CT} Rads., Sponge spicules → opal CT	Forams. → {opal CT, clinoptilolite, calcite} Rads., Sponge spicules → {opal CT, clinoptilolite}	Patches of opal CT and clinoptilolite in pore spaces	9	8	
549-44-3, 141–143	mid.–lower Albian	592.4	Laminated calcareous siltstone	Laminated siliceous fossil-bearing calcareous siltstone	Forams. → calcite Rads., Sponge spicules → opal CT	Forams. → {opal CT, clinoptilolite, calcite, pyrite} Rads., Sponge spicules → {opal CT, clinoptilolite}	Patches of opal CT and clinoptilolite in pore spaces	< 1	∞	
549-47-4, 14–17	mid.–lower Albian	621.2	Laminated calcareous sandy siltstone	Laminated very weakly silicified calcareous sandy siltstone	Forams. → only calcite Sponge spicules, Rads. → opal CT	Forams. → {clinoptilolite, opal CT} Sponge spicules, Rads. → opal CT	Patches of chalcedonic quartz	4	≈ 10	Glauconite
549-47-4, 24–26	mid.–lower Albian	621.3	Calcareous siltstone	Sparitic calcareous siltstone	Rads. → dissolved		Sparitic fine calcite cement	—	—	
550-35-5, 69–71	upper Paleocene	419.7	Siliceous marly nannofossil chalk	Nannofossil-bearing siliceous claystone	Sponge spicules, Rads., Diatoms → fresh or dissolved			—	—	
550-35-5, 87–89	upper Paleocene	419.9	Siliceous marly nannofossil chalk	Foram. marly nanno. chalk and siliceous claystone	Sponge spicules, Rads., Diatoms → partly dissolved or opal CT	Rads. → {clinoptilolite, opal CT}	Pore space → clinoptilolite	< 1	∞	
550-36-1, 12–15	upper Paleocene	422.6	Calcareous claystone	Laminated calcareous mudstone	Rads. → {dissolved or opal CT} Forams. → {clinoptilolite and opal CT}	Rads. → opal CT Forams. → opal CT	Dolomite rhombic crystals	< 1	∞	
550-36-1, 132–135	upper Paleocene	423.8	Calcareous claystone	Porcellaneous dolomite nodule	Rads. → opal CT Sponge spicules → opal CT (Forams. → only calcite)	Rads. → {quartz, opal CT} (Forams. → {quartz, opal CT})	Distinct rhombic dolomite crystals Opal CT matrix Veins of chalcedonic quartz and opal CT lep.	21	20	
550-36-2, 41–45	upper Paleocene	424.4	Calcareous mudstone	Dolomitic porcellanite nodule	Rad. → opal CT Sponges spicules → quartz opal CT (Forams. → {partly quartz})	Rads. → {opal CT, quartz} Sponge spicules → opal CT (Forams. → {opal CT, dolomite})	Opal CT matrix Rhombic dolomite crystals Veins of chalcedonic quartz and opal CT	72	13.4	

Table 5. (Continued).

Sample (interval in cm)	Chrono-stratigraphy	Sub-bottom depth (m)	Host rock	Lithology of investigated sample	Mode of occurrence of diagenetic minerals			Diagenetic silica (%)	Opal CT / Diag. Qtz	Remarks
					Fossil skeleton	Pore filling of fossil	Matrix			
550-37-1, 0–3	upper Paleocene	432.0	Nannofossil chalk	Calcareous porcellanite nodule	Rads. → {opal CT, quartz} Sponge spicules → {opal CT, quartz} Forams. → quartz	Rads. → {quartz, opal CT} Sponge spicules → {quartz, opal CT} Forams. → {quartz, opal CT}	Opal CT matrix	75	4	
550-38-6, 104–106	lower Paleocene	450.1	Nannofossil chalk	Weakly silicified siliceous fossil-bearing nannofossil chalk	Rads., Diatoms, Sponge spicules → {opal CT, clinoptilolite}	Rads., Diatoms, Sponge spicules → {opal CT, clinoptilolite}	Opal CT, Clinoptilolite → {in pore space} Dolomite rhombic crystals	23	∞	
550-39-2, 35–37	lower Paleocene	452.9	Marly nannofossil chalk	Marly siliceous nannofossil chalk	Rads., Diatoms, Sponge spicules → clinoptilolite Forams. → only calcite	Rads., Diatoms, Sponge spicules → clinoptilolite Forams. → clinoptilolite	Clinoptilolite in pore space	—	—	
551-5-2, 3–5	lower Turonian	134.0	Nannofossil chalk	Marly silicified nannofossil chalk with porcellaneous chert patches	Forams. → quartz Rads. → {opal CT lep., quartz}	Forams. → {opal CT lep., quartz} Rads. → {opal CT lep., quartz}	Microlenses or patches of chalcedonic quartz-chert with opal-CT lepisphere Opal CT	56	0.56	
551-5-2, 50–53	lower Turonian	134.5	Nannofossil chalk	Marly silicified nannofossil chalk with porcellaneous chert patches	Rads. → {opal CT, quartz}	Rads. → {quartz, opal CT}	Opal CT Microlenses or patches of chalcedonic quartz-chert bearing opal CT lep.	52	0.93	
551-5-2, 57–78	lower Turonian	134.6	Occurred at the boundary of nannofossil marly chalk and black shale	Green and black granular porcellaneous cherty mud	Rads. → {opal CT, quartz} (Forams. → calcite)	Rads. → {quartz, opal CT, clinoptilolite}	Patches of opal CT and chalcedonic quartz Clinoptilolite in matrix and also as patches Clays as matrix	45	2	Pyrite spherules
551-5-2, 79–81	lower Turonian	134.8	Black shale	Black zeolitic carbonaceous mudstone with laminations of white zeolitic clay	(Rads. → opal CT or A)	(Rads. → clinoptilolite)	Clinoptilolite as matrix and also patches Phillipsite euhedral crystals (Chalcedonic quartz patches)	≪1	—	Pyrite spherules
551-5-2, 101–103	lower Turonian	135.0	Black shale	Black zeolitic carbonaceous mudstone with laminations of white zeolitic clay	Rads. → {opal CT, quartz} Forams. → calcite only	Rads. → {quartz, opal CT}	Phillipsite euhedral crystals Clinoptilolite as matrix and also patches Clays as matrix	≪1	—	Glauconite pyrite spherules
551-6-1, 10–12	upper Cenomanian	142.2	Foram. nannofossil chalk	Foram. nannofossil chalk	Forams. → calcite only	Forams. → {opal CT, clinoptilolite}		≪1	—	
551-6-2, 82–84	upper Cenomanian	144.4	Foram. nannofossil chalk	Foram. nannofossil chalk	Forams. → calcite only	Forams. → clinoptilolite		—	—	

Notes: Where diagenetic minerals are referred to as "only calcite," no siliceous fossils were discovered. Quantities called infinite are approximations. Dashes and blanks both mean not detected by method used.

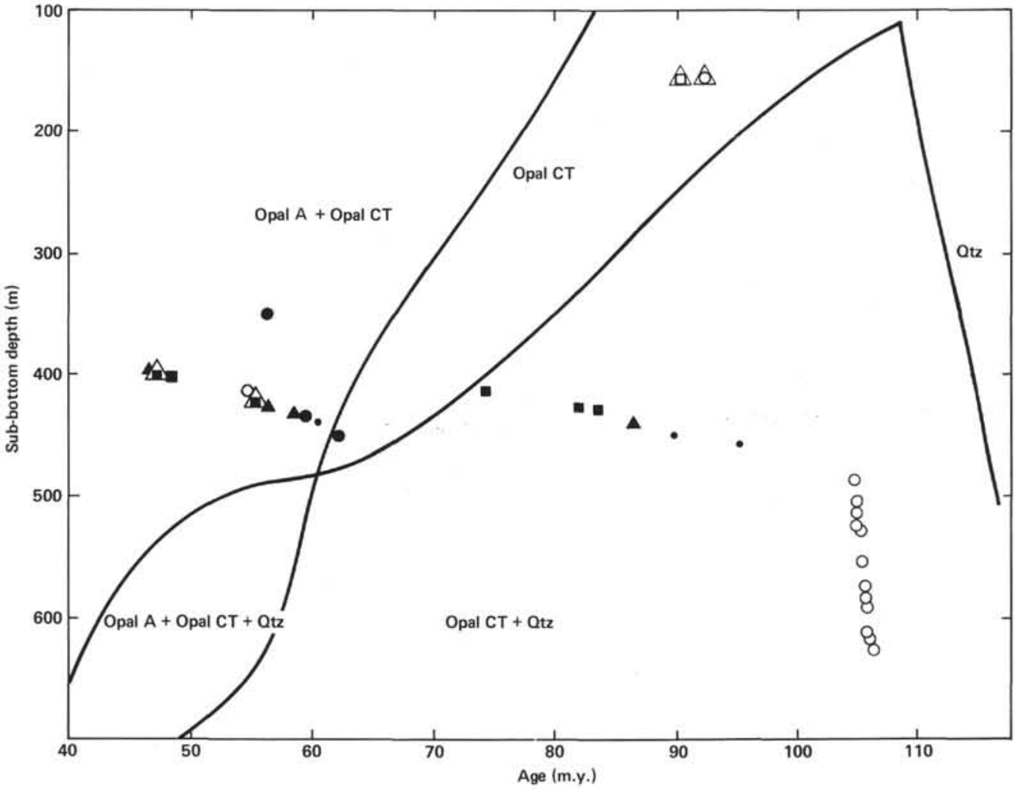

Figure 4. The relation of burial depth to sample age for the various types of silicified sediments. The fields of diagenetic silica minerals are taken from Riech and von Rad (1979a). (Symbols for silicified sediment types as in Fig. 1 legend.)

CT *d* spacings, yet indicate mature quartz chertification and a higher diagenetic quartz content. This is inconsistent with the generally accepted concept of diagenetic quartz formation after maturation or ordering of opal CT. The diagenesis of silicified sediments seems to progress more regularly with depth in the case of clayey sediments, leading to diagenetic quartz formation at deeper levels.

The most peculiar occurrence of diagenetically silicified sediments at Leg 80 sites is the discordantly shallower one in Section 551-5-2, where higher-grade diagenetically silicified sediments were recovered. This can be explained by erosion of as much as 300 m of overlying sediments at Site 551. Silicified sediments that underwent diagenesis at deeper levels are now situated close to the seafloor.

Clinoptilolite occurrences span the zones of diagenetic silica mineral formation. Riech (1980) stated, however, that clinoptilolite forms later than opal CT. The discrepancy between that statement and the Leg 80 results may indicate that the formation of clinoptilolite and the diagenesis of silica are essentially independent phenomena. Further study is necessary to resolve this question.

ACKNOWLEDGMENTS

I gratefully acknowledge the kind encouragement and support of Professor Noriyuki Nasu and Dr. Hideo Kagami of the Ocean Research Institute, University of Tokyo, during this study. On board the *Glomar Challenger*, Dr. D. Waples of Mobile Research and Development Corporation offered me some samples for XRD analysis. H. Ueda of Shizuoka University helped me with operation of the scanning-electron microscope. Dr. R. Matsumoto of the University of Tokyo gave critical comments on this paper. Dr. P. Loubere of Northern Illinois University kindly corrected the manuscript. Professor G. R. Heath of Oregon State University and Hakuyu Okada of Shizuoka University reviewed and carefully corrected the manuscript. I am greatly indebted to these people. This study has been supported by a grant-in-aid from the Ministry of Education, Science, and Culture (Monbusho) and the Japanese IPOD Committee.

REFERENCES

Garrison, R. E., Rowland, S. M., Horan, L. J., and Moore, J. C., 1975. Petrology of siliceous rocks recovered from marginal seas of the western Pacific, Leg 31, Deep Sea Drilling Project. *In* Karig, D. E., Ingle, J. C., et al., *Init. Repts. DSDP*, 31: Washington (U.S. Govt. Printing Office), 519–529.

Grehin, V. I., Pisciotto, K. A., Mahoney, J. J., and Gordeeva, S. N., 1981. Neogene siliceous sediments and rocks off southern California and Baja California, Deep Sea Drilling Project Leg 63. *In* Yeats, R. S., Haq, B. U., et al., *Init. Repts. DSDP*, 63: Washington (U.S. Govt. Printing Office), 579–593.

Heath, G. R., 1973. Cherts from the eastern Pacific, Leg 16, Deep Sea Drilling Project. *In* van Andel, T. H., Heath, G. R., et al., *Init. Repts. DSDP*, 16: Washington (U.S. Govt. Printing Office), 609–613.

Heath, G. R., and Moberly, R. M., 1971. Cherts from the western Pacific, Leg 7, Deep Sea Drilling Project. *In* Winterer, E. L., Riedel, W. R., et al., *Init. Repts. DSDP*, 7, Pt. 2: Washington (U.S. Govt. Printing Office), 991–1007.

Hein, J. R., Vallier, T. L., and Allan, M. A., 1981. Chert petrology and geochemistry, Mid-Pacific Mountains and Hess Rise, Deep Sea Drilling Project Leg 62. *In* Thiede, J., Vallier, T. L., et al., *Init. Repts. DSDP*, 62: Washington (U.S. Govt. Printing Office), 711–748.

Iijima, A., Matsumoto, R., and Tada, R., 1980. Zeolite and silica diagenesis and sandstone petrography at Sites 438 and 439 off Sanriku, northwest Pacific, Leg 57, Deep Sea Drilling Project. *In* Scientific Party, *Init. Repts. DSDP*, 56, 57, Pt. 2: Washington (U.S. Govt. Printing Office), 1143–1158.

Jones, J. B., and Segnit, E. R., 1971. The nature of opal, I. Nomenclature and constituent phases. *J. Geol. Soc. Australia*, 18:57–68.

Kagami, H., 1979. Translation of opaline silica in sediments from Bay of Biscay and Rockall Bank. *In* Montadert, L., Roberts, D. G., et al., *Init. Repts. DSDP*, 48: Washington (U.S. Govt. Printing Office), 757–764.

Keene, J. B., 1975. Cherts and porcellanites from the North Pacific, DSDP Leg 32. *In* Larson, R. L., Moberly, R., et al., *Init. Repts. DSDP*, 32: Washington (U.S. Govt. Printing Office), 429–507.

Kelts, K., 1976. Summary of chert occurrences from Line Islands Sites 314, 315, 316, DSDP Leg 33. *In* Schlanger, S. O., Jackson, E. D., et al., *Init. Repts. DSDP*, 33: Washington (U.S. Govt. Printing Office), 855–863.

Lancelot, Y., 1973. Chert and silica diagenesis in sediments from the central Pacific. *In* Winterer, E. L., Ewing, J. I., et al., *Init. Repts. DSDP*, 17: Washington (U.S. Govt. Printing Office), 377–405.

Mitsui, K., 1975. Diagenetic alteration of some minerals in argillaceous sediments in western Hokkaido, Japan. *Sci. Rep. Res. Inst. Tohoku Univ.*, 13:13–65.

Murata, K. J., and Larson, R. R., 1975. Diagenesis of Miocene siliceous shales, Temblor Range, California. *J. Res. U.S. Geol. Surv.*, 3:553–566.

Pisciotto, K. A., 1980. Chert and porcellanite from Deep Sea Drilling Project Site 436, northwest Pacific. *In* Scientific Party, *Init. Repts. DSDP*, 56, 57, Pt. 2: Washington (U.S. Govt. Printing Office), 1133–1142.

Riech, V., 1979. Diagenesis of silica, zeolites and phyllosilicates at Sites 397 and 398. *In* von Rad, U., Ryan, W. B. F., et al., *Init. Repts. DSDP*, 47, Pt. 1: Washington (U.S. Govt. Printing Office), 741–759.

________, 1980. Diagenesis of siliceous sediments, porcellanites, and cherts of the Moroccan Basin, Deep Sea Drilling Project Sites 370, 415, and 416. *In* Lancelot, Y., Winterer, E. L., et al., *Init. Repts. DSDP*, 50: Washington (U.S. Govt. Printing Office), 725–731.

________, 1981. Siliceous sediments from the Nauru Basin: diagenetic alteration of biogenic opal and authigenesis of silica and silicates. *In* Larson, R. L., Schlanger, S. O., et al., *Init. Repts. DSDP*, 61: Washington (U.S. Govt. Printing Office), 523–531.

Riech, V., and von Rad, U., 1979a. Silica diagenesis in the Atlantic Ocean: diagenetic potential and transformations. *In* Talwani, M., et al. (Eds.), *Deep Drilling Results in the Atlantic Ocean: Continental Margins and Paleoenvironment*. Am. Geophys. Union, Maurice Ewing Series 3:315–340.

________, 1979b. Eocene porcellanites and Early Cretaceous cherts from the western North Atlantic Basin. *In* Tucholke, B. E., Vogt, P. R., et al., *Init. Repts. DSDP*, 43: Washington (U.S. Govt. Printing Office), 437–455.

von Rad, U., Riech, V., and Rosch, H., 1978. Silica diagenesis in continental margin sediments off northwest Africa. *In* Lancelot, Y., Seibold, E., et al., *Init. Repts. DSDP*, 41: Washington (U.S. Govt. Printing Office), 879–905.

Date of Initial Receipt: January 28, 1983
Date of Acceptance: November 23, 1983

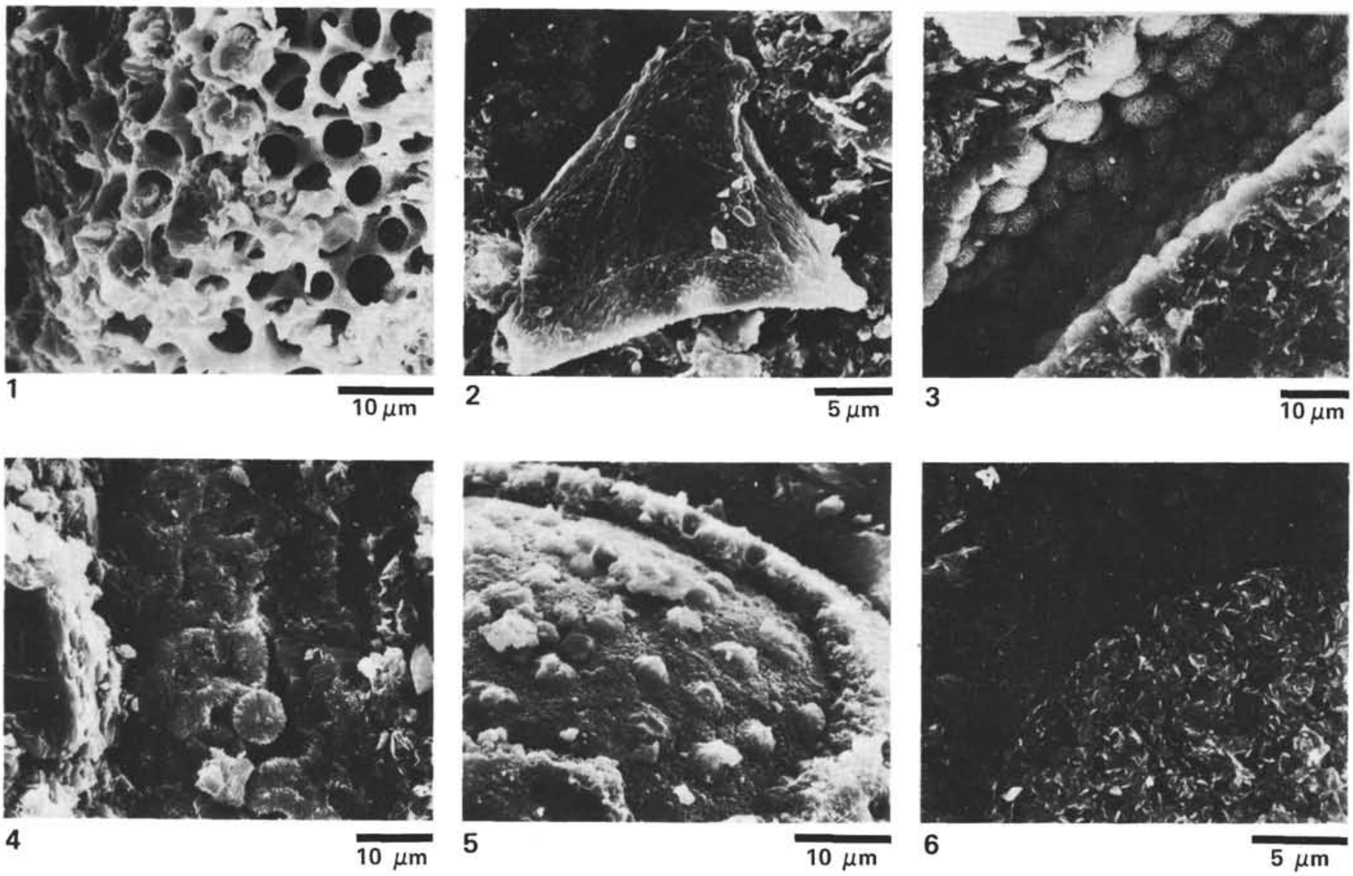

Plate 1. Scanning-electron micrograph of silica diagenetic change of biogenic skeletons and precipitation of silica minerals in pore spaces. **1.** Sample 549-18-2, 96–99 cm (upper Paleocene, sub-bottom depth 353 m, ×2200), well-preserved radiolarian skeleton, almost fresh but weakly dissolved. **2, 6.** Sample 548A-21-2, 133–136 cm (middle Eocene, sub-bottom depth 398 m), (2) ×3600, a fragment of sponge spicule with distinct dissolution pits on the surface, (6) ×4400, foraminiferal test replaced by quartz, with sediment filling the inner pore space. **3.** Sample 549-35-1, 37–39 cm (middle Albian, sub-bottom depth 512 m, ×1500), opal-CT lepispheres precipitated as thin wall, probably on the trace of sponge spicule. **4.** Sample 549-42-2, 38–40 cm (lower Albian, sub-bottom depth 571 m, ×1800), opal-CT lepispheres precipitated in pore space in clayey sediment matrix. **5.** Sample 549-32 (top), top-situated nodule (middle Albian?, sub-bottom depth 484 m, ×2200), diagenetic quartz precipitated in the pore space of a foraminifer, the mold of the inner texture clearly evident.

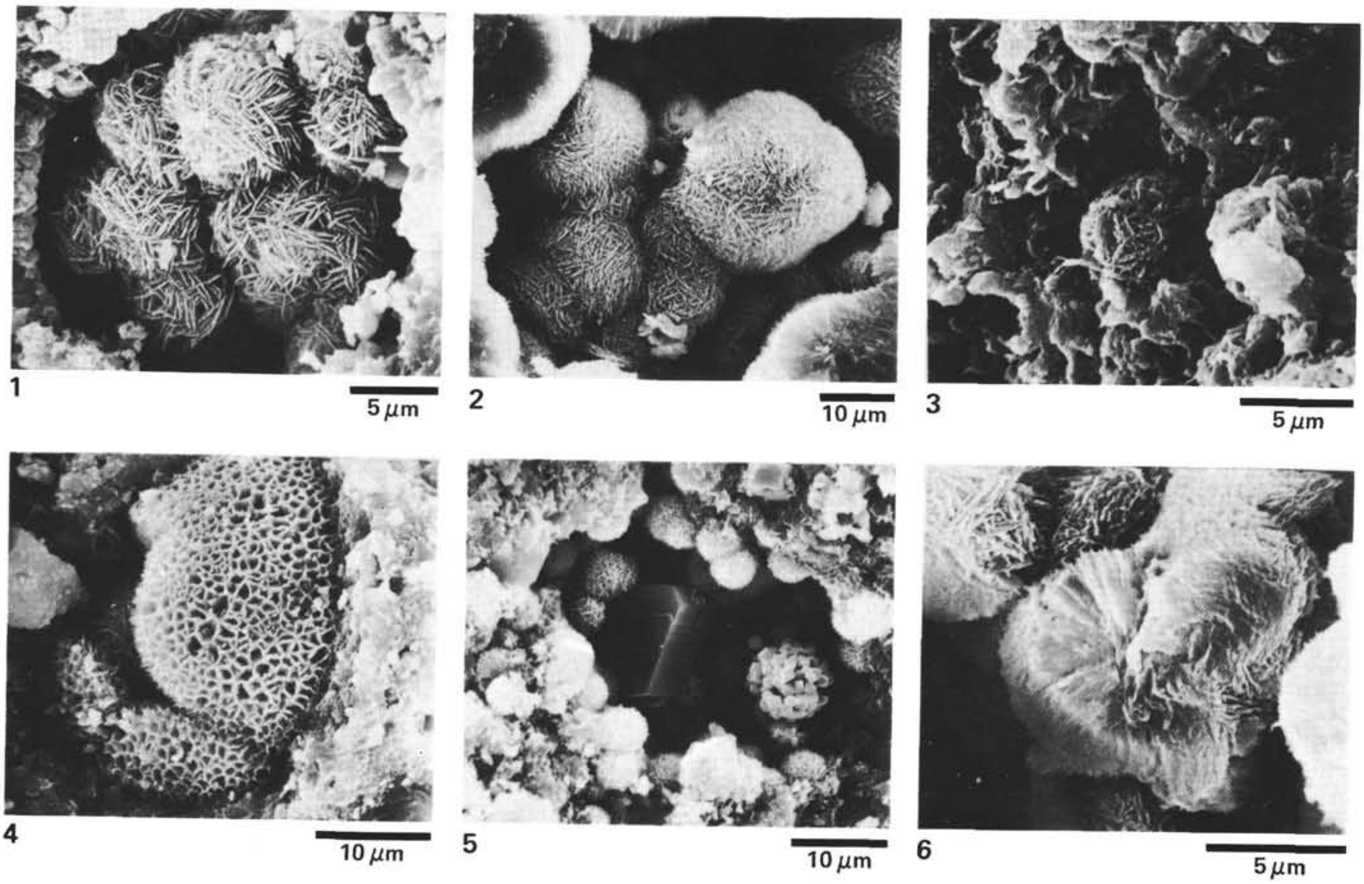

Plate 2. Opal-CT lepispheres in pore spaces of fossils and matrix. **1.** Sample 548A-21-1, 56–59 cm (middle Eocene, sub-bottom depth 396 m, ×4400), opal-CT lepispheres in a foraminiferal test. **2, 4.** Sample 549-32 (top), top-situated nodule (middle Albian?, sub-bottom depth 484 m), (2) ×1800, large opal-CT lepispheres in pore space of matrix, (4) ×2600, opal-CT lepispheres in pore space of a foraminiferal test. **3.** Sample 551-5-2, 3–5 cm (lower Turonian, sub-bottom depth 134 m, ×5400), opal-CT lepisphere in calcareous matrix. **5.** Sample 549-42-2, 38–40 cm (lower Albian, sub-bottom depth 571 m, ×2200), opal-CT lepispheres, euhedral crystal of calcite, and framboidal pyrite crystal aggregates in pore space of clayey siltstone. **6.** Sample 549-35-1, 37–39 cm (middle Albian, sub-bottom depth 512 m, ×1500). A section of opal-CT lepispheres can be seen in clayey siltstone matrix.

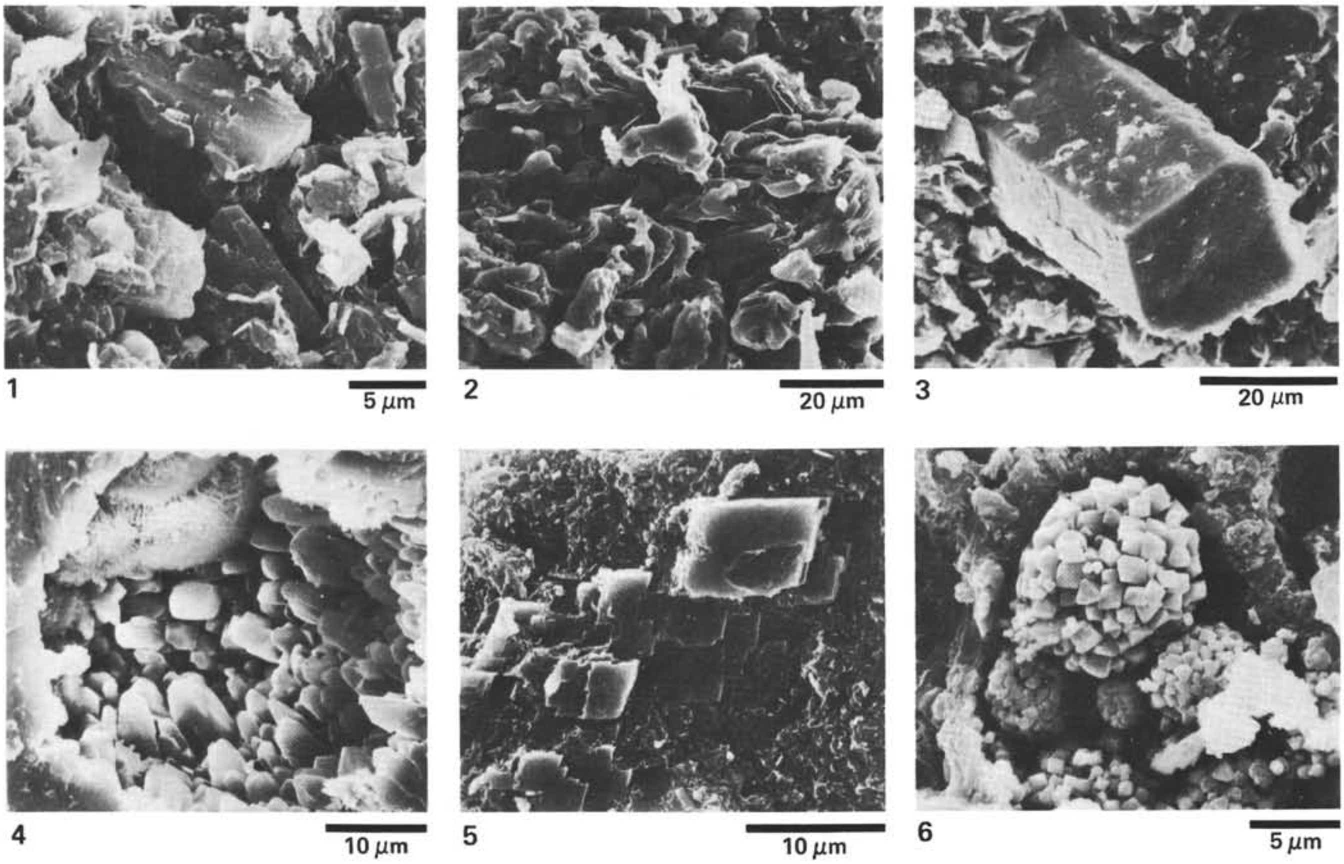

Plate 3. Authigenic zeolites and other diagenetic minerals in silicified sediments. **1-3.** Sample 551-5-2, 79–81 cm (lower Turonian, sub-bottom depth 135 m), (1) ×3600, clinoptilolite crystals in matrix of tuffaceous? chalk, (2) ×1260, dissolved clinoptilolite crystals in matrix of tuffaceous chalk, (3) ×1600, euhedral phillipsite crystal in matrix of clinoptilolite and clay minerals. **4.** Sample 549-32 (top), top-situated nodule (middle Albian?, sub-bottom depth 484 m, ×2400), opal-CT lepispheres and authigenic calcite crystals in void of a foraminiferal test. **5.** Sample 550-36-1, 132–135 cm (upper Paleocene, sub-bottom depth 424 m, ×3200), dolomite rhombic euhedral crystals in opal CT and clay matrix in dolomitic porcellanite nodule. **6.** Sample 548A-21-1, 56–59 cm (middle Eocene, sub-bottom depth 396 m, ×4000), framboidal pyrite crystal aggregates in foraminiferal chamber in porcellanite nodule. The chamber wall has been replaced by opal CT.